coatings

MDPI

Article

Durable Flame-Resistant and Ultra-Hydrophobic Aramid Fabrics via Plasma-Induced Graft Polymerization

Eshraga A. A. Siddig [1,2], Yu Zhang [1], Baojing Yang [3], Tianshu Wang [3], Jianjun Shi [1,4,5], Ying Guo [1,4,5], Yu Xu [1,*] and Jing Zhang [1,4,5,*]

1 New Energy Material and Device, College of Science, Donghua University, Shanghai 201620, China; eshragashining@gmail.com (E.A.A.S.); 2161508@mail.dhu.edu.cn (Y.Z.); jshi@dhu.edu.cn (J.S.); guoying@dhu.edu.cn (Y.G.)
2 College of Engineering, Sudan University of Science and Technology (SUST), Khartoum 11111, Sudan
3 Precision Chemical Technology (Shanghai) Co., Ltd., Shanghai 201613, China; 18967138899@189.cn (B.Y.); 18964959992@126.com (T.W.)
4 Textile Key Laboratory for Advanced Plasma Technology and Application, China National Textile & Apparel Council, Shanghai 201620, China
5 Magnetic Confinement Fusion Research Center, Ministry of Education of the People's Republic of China, Shanghai 201620, China
* Correspondence: yuxu@dhu.edu.cn (Y.X.); jingzh@dhu.edu.cn (J.Z.)

Received: 28 October 2020; Accepted: 5 December 2020; Published: 18 December 2020

Abstract: A durable flame-resistant and ultra-hydrophobic phosphorus–fluoride coating on aramid fabrics was achieved by plasma-induced graft polymerization. The aramid fabrics were activated and roughed through the low-pressure plasma firstly, which involves the sequential coating of a mixture of phosphorus–fluoride emulsion copolymer. When potentially exposed to flame or water, such a surface produces a dual effect in which it is intumescent and waterproof, successfully giving the coated fabrics flame-resistant ultra-hydrophobic bifunctional properties. Thus, adhesive coatings provide a convenient way to resolve the issue of washing durability of the coatings. The as-prepared fabrics last for 10 repeatable washing cycles without losing their flame resistance and superhydrophobicity, suggesting future applications as advanced multifunctional textiles. Compared to an untreated coating, its char length was less than 1 cm with no measurable after-flame or after-glow times, and its static water contact angle remained stable above 170°. Meanwhile, the control sample was unable to extinguish the fire with a damage length of 10.6 cm and a water contact angle of 100°. All the results indicate that plasma-reactive polar groups interact between phosphorus and fluorine elements, leading to an increased relative atom ratio P and F through Energy-Dispersive Spectrometer (EDS) spectra and XPS analysis, which inhibits the flammability and wettability.

Keywords: plasma polymerization; phosphorus-fluoride coating; flame-resistant; hydrophobic; washing durability

1. Introduction

High-performance textiles, including the exploration of multifunctional textiles that protect humans from environmental hazards and threats (chemicals, fire, water, oils, gases, and pollution, etc.) such as firefighter apparel, medical, and military garments, have a highly desirable quality standard [1,2]. Potential applications in various areas have made impressive efforts to develop new functionalization fibers and/or textiles that provide multiple mechanisms of protection with their intrinsic properties [3]. However, most protection requires unique and interface function fabrics,

which made aramid fabrics, including Kevlar, Armos, and Twaron, the right choice due to their high strength and modulus, high temperature and alkali resistance, and lightweight as multiple protection performance textiles [4,5]. Unfortunately, the adhesion between aramid fibers and most matrices is severe in introducing multiple coatings as a result of the compact molecule structure, high crystallinity, and smooth surface [6,7]. Surface modification eventually adds new functionalities to the material and incorporates functional components for multiple features without modifying the textile's intrinsic properties [8–10]. In recent years, researchers have produced various flame resistance and hydrophobic coatings on fabric surfaces. Chen et al. [11] achieved superhydrophobic, self-cleaning, and heat resistance on cotton fabric by using solution-dipping methods involving the sequential deposition of branched poly(ethylenimine), ammonium polyphosphate, and a fluorinated polyhedral oligomeric silsesquioxane trilayer. Zhang et al. [12] synthesized phosphorus–nitrogen–silicon with flame-retardant waterborne polyurethane (FRWPU) combined with cyclic lateral phosphoramidites and a post-chain extension process. The Wei group fabricated flame-retardant and hydrophobic multifunctional cotton fabrics [13]. However, these methods continue to have certain disadvantages, such as complex and long-term operations and the use of toxic compounds; furthermore, the coating durability is limited [14–17].

Generally, the organic coating on fabric surfaces is inherently fragile to mechanical forces, and the fabric has to suffer repeated washing during the fabric's lifetime [18,19]. In consideration of environmental, green chemistry issues, and adhesive coatings, the Environmental Protection Agency's (EPA and KO-TEX Standard100) requirement for C8 replacement, with C6 fluorine or a non-fluoride hydrophobic agent, is the primary strategy to endow them with hydrophobicity. C6 or free-fluorine hydrophobic agents struggle because of their environmental and ecological issues [20]. The phosphorus component has been recognized for its high efficiency of flame retardants, excellent smoke reduction, and eco-friendly benefits [21]. Given those facts, multifunctional fabrics are challenging to confer two or more properties, simultaneously anti-flammable and water repellent, and washing durability with a minimum number of treatment stages.

Plasma, recognized for its high concentrations of energetic species and the chemical reactions, has long been used to enhance the adhesion properties of aramid fiber-reinforced composites [2,22,23]. Consequently, plasma graft polymerization coatings are considered to be the most effective technology for the production of high-performance fabrics [24]. The fiber surface topography changes during plasma treatment by oxidized etching of the dissociated polymer molecular chains and chemically react together with a polymerization scheme of ring-closure, which then propagates the response by combining dip-coating or cross-linking multifunctional units [25,26].

In this work, we developed a functional technique to obtain a durable flame-resistant ultra-hydrophobic coating on aramid fabrics through plasma roughness and activation firstly and then subsequently applying a coating of phosphorus–fluoride emulsion copolymer on aramid fabric by plasma graft polymerization. The reactive phosphorus–fluoride coating with a mixture of organophosphorus component and C6 fluorine awarded a durable flame-resistant ultra-hydrophobic property to the textile depending on the fiber's plasma surface activation surface, which was a benefit for the diffusion and adhesion of the phosphorus–fluoride coating. The plasma graft polymerization technology, which is desirable for processing textiles, supports a faster continuous treatment of materials with excellent potential and practical applications in fabricating durable bifunctional synthetic polymers.

2. Materials and Methods

Poly-phenylene terephthalamide (PPTA, Wujiang Shengxu Textile Co.,Ltd., Wujiang, China) aramid fabrics were weighted (average 7.85 g) and cleaned for 30 min at 100 °C in a water bath. Argon and oxygen (purity 99.99%, Cheng Gong Gas Industry Co., Ltd., Shanghai, China) were used for the plasma-treating process. The coating emulsion was a combination of C6 fluorine and an organophosphorus component individually supplied by Precision Chemical Technology Co., Ltd., Shanghai, China.

2.1. Plasma Surface Modification

A capacitively coupled radio frequency low-pressure plasma system operated at 13.56 MHz was used for surface activation of the fabric shown in our previous research [27]. To obtain a significant rough surface, the experimental parameters were optimized. A mixture gas of Ar (10 sccm) and O_2 (90 sccm), 300 W power supply, and 300 s treating time were used in the plasma treating process.

2.2. Phosphorus–Fluoride Coatings on Aramid Fabric Surface

The fabrics were submerged in a mixture of C6 fluorine (20%, *w*/*w*) and organophosphorus component (30%, *w*/*w*) that was vigorously stirred at room temperature; then, using a Pad-Dry-Cure method containing two rubber-covered pad rollers with a 3.5 rapid (speed of the rollers), they were subsequently dried at 190 °C for 150 s. To obtain the more desired properties, the selection of observable coating variables, mixture concentration ratio, and rapid rollers, as well as temperature and time were consistent with the experimental work. After that, all fabrics were rinsed with distilled water to extract waste chemicals. The possible chemical reaction between the mixture and aramid fabric is presented in Scheme 1. Final materials were assigned as untreated coated (UC) and plasma-treated coated (PC). Moreover, the untreated (original, referred to as U) and the plasma-treated (referred to as P) conditions are shown in Table 1.

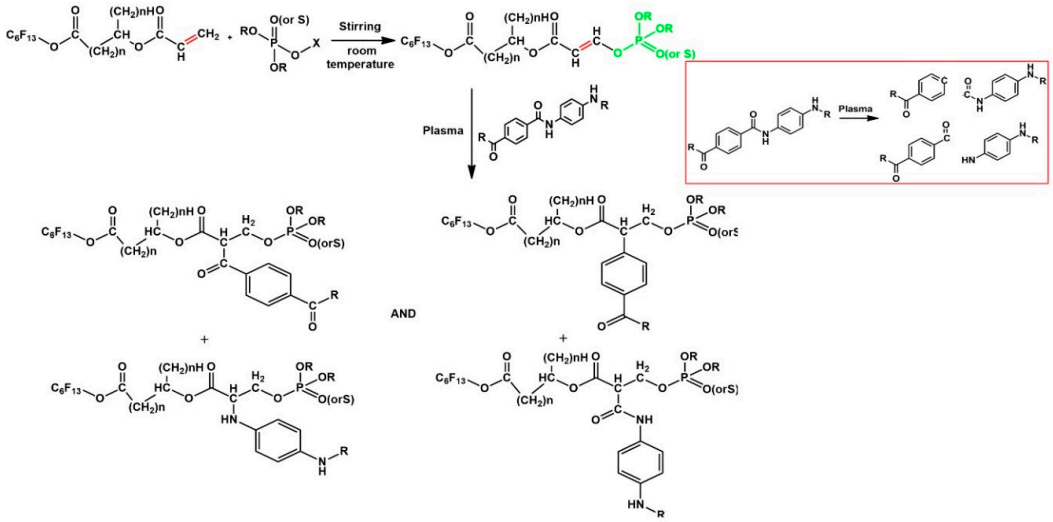

Scheme 1. Possible chemical reactions on aramid fabric.

Table 1. The sample names used in the experiment.

Experimental Conditions	Treatment Formulas	Coating Formulas	Washing Cycles Formulas		
			1 (Time)	5 (Time)	10 (Time)
Untreated	U	UC	UCW_1	UCW_5	UCW_{10}
Plasma treated	P	PC	PCW_1	PCW_5	PCW_{10}

2.3. Coating Durability Test

The coating durability was evaluated by subjecting the untreated coated (UC) and plasma-treated coated (PC) fabrics to a repeatable series of 10 washing cycles; each washing cycle was performed for 1 h with (11 g) regular soap and dried for 1 h in a furnace at 60 °C, according to AATCC standard. Table 1 listed the names of samples with specific washing cycles.

2.4. Fabric Surface Analysis

Atomic Force Microscopy (AFM, Multimode Nanoscope III a, Digital Instrument, Santa Barbara, CA, USA) was used to calculate the surface roughness by two parameters, the mean square root (RMS)

and the average roughness (Ra). The surface topography analyzed by Field Emission Scanning Electron (FE-SEM, S-4800, Hitachi Ltd., Tokyo, Japan) fitted with Energy-Dispersive Spectrometer (EDS) for elemental mapping analysis. Attenuated Total Reflection-Fourier Infrared Spectrometer (ATR-FTIR, Nicolet 6700, Thermo Fisher Scientific, Madison, WI, USA) was recorded in the range of 500–4000 cm^{-1} to measure the chemical bonding. The chemical compositions were elaborated by X-ray photoelectron spectroscopy (XPS, Shimadzu-Kratos, Axis Ultra DLD, Kyoto, Japan) calibrated at binding energy (BE) 284.8 eV. Thermogravimetric Analysis (TGA, 1201C) was carried out to identify the degradation and weight variation under a flow rate of N_2 atmosphere (50 mL min^{-1}) from 600 °C ambient temperature at a heating rate of 10 °C per minute.

The superhydrophobic behavior was analyzed by a Drop Meter A-200 (MALSI, Guangzhou, China) water contact angle. For practical application, the resistance of fabrics to fire behavior was conducted using the vertical flame test (GB/T 5455).

3. Results and Discussion

3.1. Surface Characterization

The topographical modifications of the surface were examined using AFM images. Figure 1a shows the untreated aramid fabric after coating and washing U, UC, and UCW_{10}, respectively. The U surface is relatively smooth and flat with a surface roughness (Ra) value of 2.52 nm, while the coating of the UC surface was partially covered with hill shapes that raised the Ra value to 19.30 nm, which continuously diminished to 1.94 nm for UCW_{10}. Plasma treating, coating, and 10 times washing are shown in Figure 1b for P, PC, and PCW_{10}, respectively. Small pits formed with a surface roughness of 20.83 nm on the P surface. Considering PC, the topography changes to a random distribution of micro-sized protuberances, and hills relatively increased the surface roughness to 35.6 nm. Plasma etching enables the removal of atoms and molecules from the fiber surface; thus, it increased the roughness of the surface [28,29]. After washing PCW_{10} 10 times, there was only a slight decrease in the roughness value: 31.3 nm.

The surface of the untreated phosphorus–fluoride coating (UC) is shown in the SEM image in Figure 2a; the fiber surface was only partially covered with bulger shapes. Figure 2c shows that the shapes made of C, O, N, F, and P elements with relative atom ratios (At) of 34.6%, 29.8%, 6.6%, 10.1%, and 14.2%, respectively, were recognized. After plasma treatment and coating PC, the fiber surface presents a completely coved thick rough layer with dots, as shown in Figure 1b. The EDS results show in Figure 2d that the ratios of C, O, N, F, and P were higher than UC, which are 26.4%, 36.2%, 7.1%, 11.5%, and 15.6%, respectively. The plasma etching process created rough surfaces and introduced a large number of reactive radicals or groups. The rough surface becomes attractive to phosphorus and fluorine molecules, resulting in improved absorption and penetration on the fabric surface. Therefore, the durability increased for the better coating adhesion formed on the plasma pre-treated surfaces [30].

After 10 times washing, the phosphorus–fluoride coating is seriously flaked from the UCW_{10} fiber surface, as seen in Figure 3a. The EDS spectra analysis in Figure 3c confirms that the relative surface atomic ratios of phosphorus–fluoride coating decreased to P (0.00%) and F (3.8%), while C (39.9%), O (25.8%), and N (4.7%) change little. The coating was largely preserved on the PCW_{10} fiber surface, and only slight differences were observed, as shown in Figure 3b. A slight washing effect in the energy spectrum ratios is shown in Figure 3d. These results implied that plasma pre-treatment had enhanced the adhesion of the coating to the fabric.

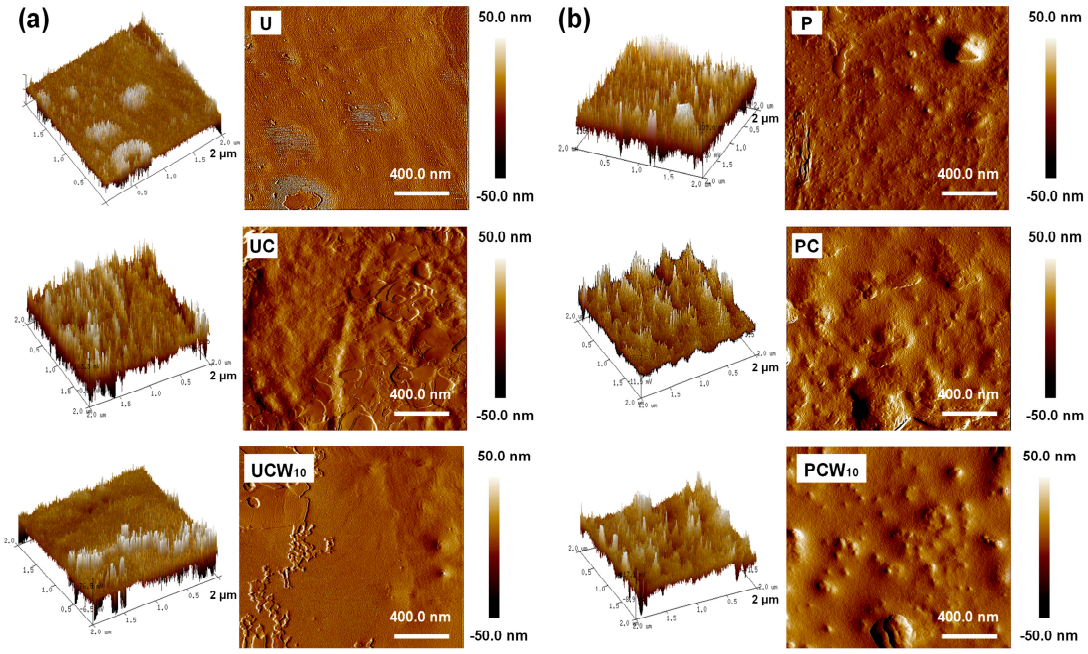

Figure 1. Atomic Force Microscopy (AFM) images of aramid fabric after various treating, coating, and washing processes. (**a**) Untreated (U), untreated phosphorus–fluoride coating (UC), and UC with 10 washing cycles (UCW_{10}); (**b**) plasma-treated (P), plasma-treated coated (PC), and PC with 10 washing cycles (PCW_{10}).

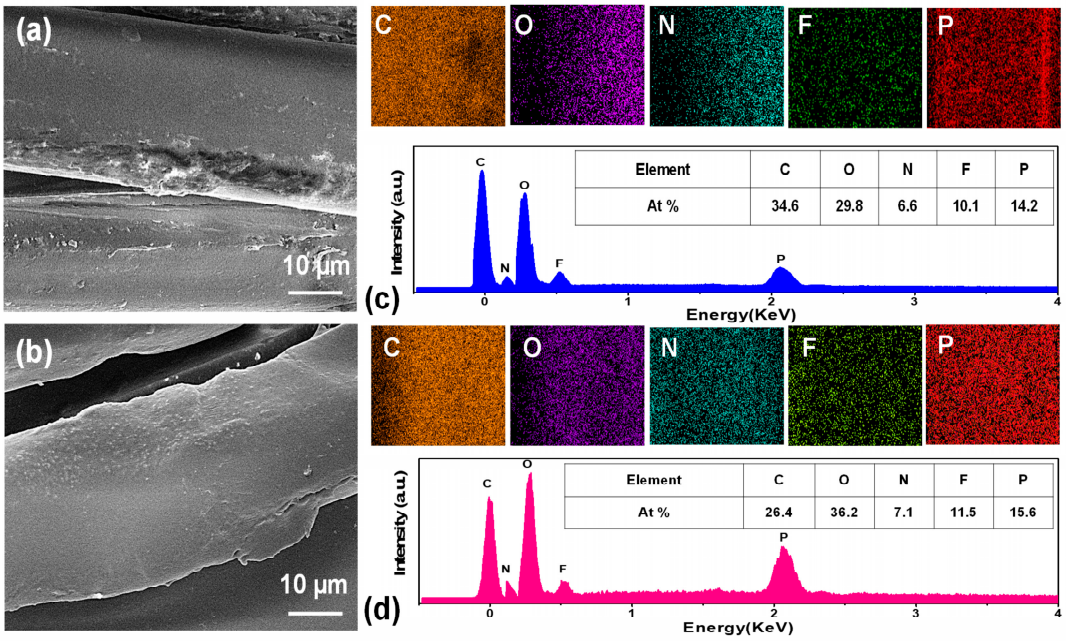

Figure 2. The SEM and Energy-Dispersive Spectrometer (EDS) element mapping with their atomic ratio (At) table (inset) of aramid fabric after coating (**a**,**c**) for UC and (**b**,**d**) for PC, respectively.

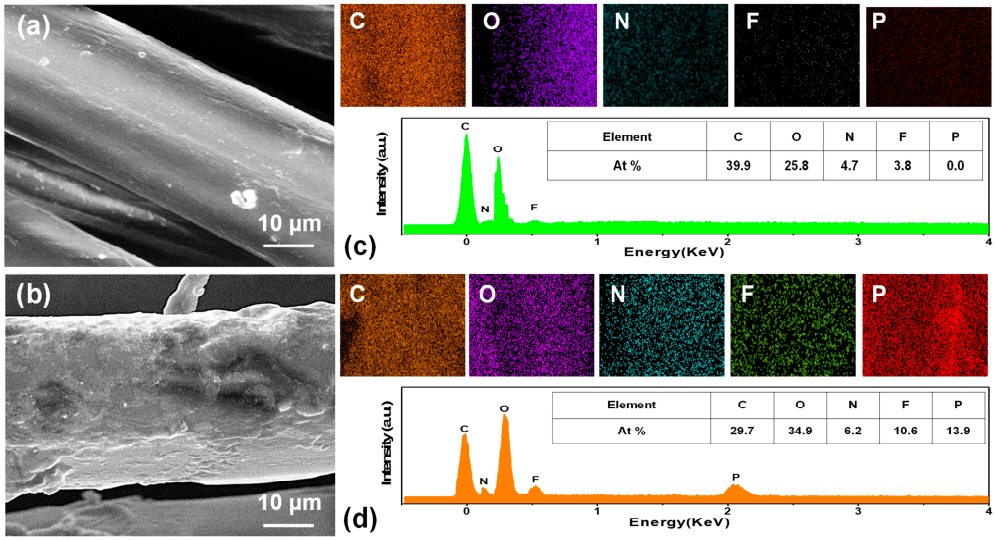

Figure 3. The SEM and EDS element mapping with their atomic ratio (At), table (inset) of aramid fabric after coating, and 10 times washing (**a**,**c**) for UCW_{10} and (**b**,**d**) for PCW_{10}, respectively.

3.2. Phosphorus–Fluoride Graft Polymerization Reactions

ATR-FTIR analysis was used to describe the functional group's reactions to confirm the phosphorus–fluoride bonding status onto aramid fabric. The characteristic bands at 3292, 2921, 1412, and 1240 cm^{-1} were observed in pristine aramid fabric [31]. Figure 4 shows the characteristic groups at 1740, 1240, 1015, and 906 cm^{-1} attributed to C=O/–CF=CF_2, C–H/C–F, P–O–C, and P–O, respectively. Among the bands, the stretching vibration at 1740 cm^{-1} and 1240 cm^{-1} were in the range of the C-F stretches in aliphatic fluoro-compounds; this indicates that C6 fluorine copolymer was bound to the fabric surface [32,33]. Meanwhile, the bands at 1015 cm^{-1} and 906 cm^{-1} confirm the organophosphorus component coating [10,34,35]. The higher peaks indicate that the plasma pre-treatment coating introduces more phosphorus–fluoride compounds than the direct (untreated) coating; after repeating washing cycles, the strong presence of a phosphorus–fluoride coating on plasma-treated samples PCW_1 and PCW_{10} evidence the adhesion bonding strength, which acts on the interfacial bonds between the coating solution and the fabric surface, confirming that plasma graft polymerization introduces more phosphorus–fluoride compounds and is not affected by washing compared with direct coating as displayed in Figure 4a, for UC, UCW_1, and UCW_{10}, and Figure 4b for PC, PCW_1, and PCW_{10}, respectively.

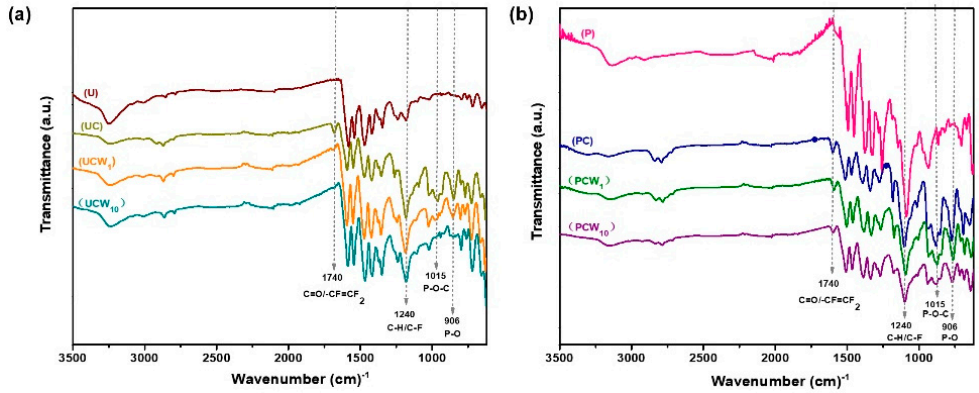

Figure 4. Attenuated Total Reflection-Fourier Infrared Spectrometer (ATR-FTIR) spectrum of aramid fabric samples after various coating and washing processes: (**a**) U, UC, UCW_1, and UCW_{10}, and (**b**) P, PC, PCW_1, and PCW_{10}.

The plasma graft polymerization reactions of the phosphorus–fluoride coating on the fabrics were described by X-ray photoelectron spectroscopy (XPS), and it was coinciding with EDS and FTIR results. Figure 5 shows the high-resolution spectra of O1s, F1s, and P2p for untreated coating UC and plasma-treated coating PC fabrics. The primary O1s range in Figure 5a consists of two peaks at 531.8 eV for CONH and 534.7 eV for CO(O)H, which might be associated with O–F and O=P, and this suggested that the proportionate of phosphorus–fluoride coating occurs in the conversion process [36]. The core level F1s shown in Figure 5b can be fitted to two peaks CF_3 and CF_2 [37]. Carbon–fluorine bonds, which react with the reactive plasma group in the material's precocious covalent bonds CF_3 before the CF_2 unit, shifted PC to higher bonding energy [38]. For the P2p spectrum in Figure 5c composed of PO_4, the ionization state seized oxygen more than PO_3 [39,40].

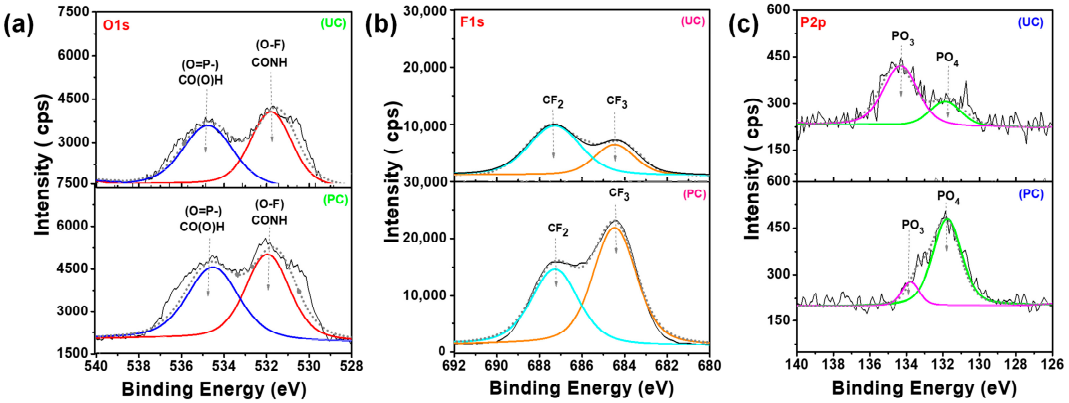

Figure 5. Deconvoluted XPS spectra of untreated phosphorus–fluoride coating UC and plasma-treated and phosphorus–fluoride coating PC on aramid fabric (**a**) O1s, (**b**) F1s, and (**c**) 2p, respectively.

In Figure 6, after 10 times washing, UCW_{10} and PCW_{10} fabrics, it can be observed that the intensities of the peaks were higher in PCW_{10}. Moreover, the increased amount of the relative atom ratios in PCW_{10} of O1s, F1s, and P2p shown in Table 2 confirm that plasma pre-treatment samples were unaffected by washing. The results suggested that the plasma-activated aramid surface improved the graft polymerization of phosphorus–fluoride emulsion molecules [41].

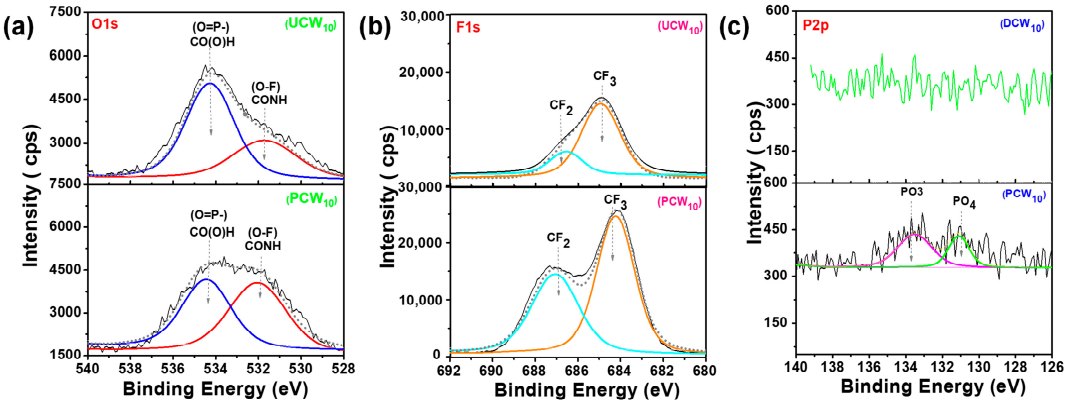

Figure 6. Deconvoluted XPS spectra of untreated phosphorus–fluoride coating UCW_{10} and plasma-treated and phosphorus–fluoride coating PCW_{10} after 10 times washing on aramid fabric (**a**) O1s, (**b**) F1s, and (**c**) P2p, respectively.

Table 2. Surface elements of aramid samples by XPS.

Samples Names	Atomic Ratio (%)			
	C1s	O1s	F1s	P2p
UC	43.2	9.8	54.5	1.6
UCW_{10}	37.9	5.7	41.7	0.3
PC	36.5	10.5	79.7	3.1
PCW_{10}	33.8	9.6	76.9	2.9

TGA curves were carried out to investigate the thermal degradation mechanism of aramid fabrics before and after coating and washing. Figure 7a reports the major degradation observed at 448.97 °C, weight 92.9% for untreated aramid U fabric because of the aromatic and aliphatic amine hardener decomposition [42,43]. The plasma-treated P fabric's TG curve shifted to the left and overlapped with the U fabric at (445.58 °C, 92.5%) due to plasma treatment catalyzing the degradation process depending on the plasma etching time, which neutralizes the clay delaying effect [24]. Figure 7b shows that the thermogravimetric analyses show that the coatings improved the aramid fabric thermal stability [44]. Furthermore, when samples suffered from heat, the UC fabric pyrolyzed at (444.89 °C, 86.4%) earlier than the PC sample at (448.87 °C, 90.0%), propelling the generation of intumescent char layers. Finally, in Figure 7c, after washing, the degradation curve for UCW_{10} at (440.30 °C. 85.8%) and PCW_{10} at (447.03 °C, 89.7%) conform, and the plasma-treated fabric surface was covered by a layer of continuous and compact char. The plasma polymerization with a phosphorus–fluoride coating made a little barrier-protecting layer from the thermal radiation, suppressed the gas release and reduced the matrix decomposition rate [35,45]. The high degradation temperature of aramid fibers and inorganic materials usually melt before they decompose. Therefore, there were no significant changes in the weight loss. The characteristic temperatures TGA and DTG are presented in Table 3.

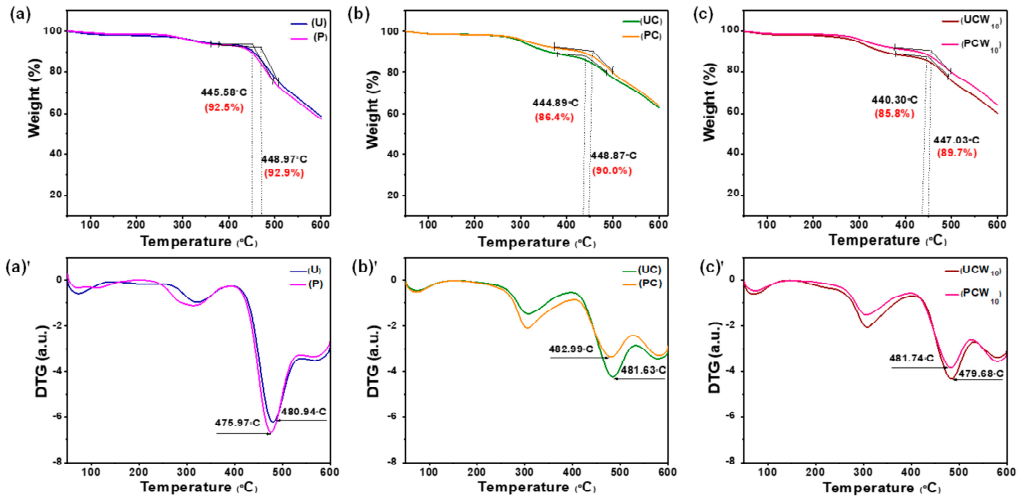

Figure 7. TGA and DTG curves of aramid fabric samples after various treating, coating, and washing processes: (**a**,**a**′) U and P, (**b**,**b**′) UC and PC, (**c**,**c**′) UCW_{10} and PCW_{10}.

Table 3. Thermogravimetric Analysis (TGA) and DTG data of aramid samples obtained in N_2 atmosphere.

Sample Name	TGA (°C)	Weight (%)	DTG (°C)
U	448.97	92.9	480.94
UC	444.89	86.4	481.63
UCW_{10}	440.30	85.8	479.68
P	445.58	92.5	475.97
PC	448.87	90.0	482.99
PCW_{10}	447.03	89.7	481.74

3.3. Durable Flame-Resistant Ultra-Hydrophobic Performance

In order to evaluate the flame-resistant visually during burning, a vertical flame test (GB/T 5455) was employed [46]; since the LOI test was based on the material property, for most polymeric fabric, it varies from 18 to 22% [47–49]. In Figure 8a, after exposure to flames for 12 s, it is clear that the untreated samples, U, UC, UCW_1, UCW_5, and UCW_{10}, were unable to extinguish the fire, leaving damaged surfaces with char length continuously increased with repeating washing cycles. As for plasma-treated fabric, the burnt region was still smoldering and slowly charred. Meanwhile, after coating and washing, all plasma-treated fabric showed no observable after-flame or after-glow times, and char lengths were also not noticeable. It was remarkable that the plasma polymerization fabrics self-extinguished the fire quickly with no after-flame or smolder. Regarding the flame test, the fabric maintained its solidity with less than 1 cm char length. The results showed that the phosphorus–fluoride coating on plasma pre-treated surfaces had an outstanding durable flame resistance effect by isolating the fabrics effectively from burning, heat, and flammable gases. This occurs through the flame-retardant coated layer dehydrating action, generating a double bond in the polymer to form a carbonaceous layer via cyclizing and the cross-linking cycle, which had intumescence and shielded the fabric from the heat of the flame.

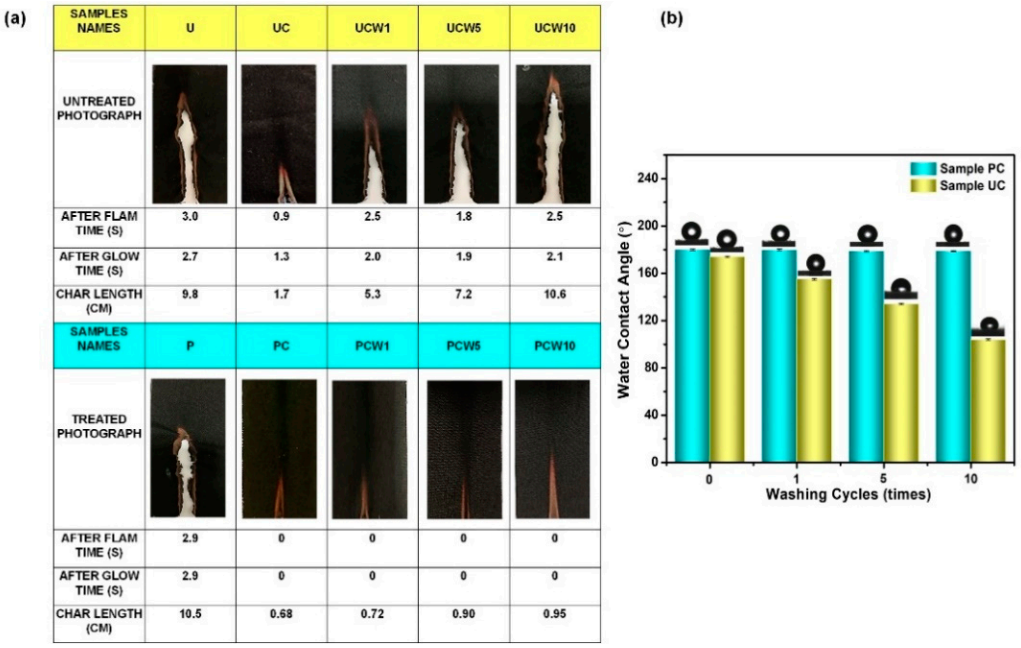

Figure 8. The vertical flammability test and water contact angles of untreated and plasma-treated after coating and repeating washing on aramid fabric surfaces: (**a**) vertical flammability standard photographs on untreated and plasma-treated fabrics, respectively, (**b**) water contact angles and their corresponding graph vs. washing cycles.

The hydrophobicity of fabrics was studied by the water contact angle technique before and after repeated washing cycles, as shown in Figure 8b. The water contact angle of untreated coated UC was 166° and continuously decreased after repeated washing cycles. However, after the plasma coating, PC showed a remarkably increased hydrophobicity with a water contact angle as high as 179.9°. Further, after repeated washing, the water contact angle remained stable, which means that the durable superhydrophobic coating formed on the plasma polymerization fabrics.

As shown above, the plasma pre-treatment increased the surface roughness and introduced reactive groups on aramid fabric surfaces, which is beneficial for preparing the durable flame-resistant ultra-hydrophobic surface. Moreover, the surface physical chemistry changes made the fabric absorb

more phosphorus–fluoride coating and improved its adhesion on the surface, which greatly enhanced the washing durability of the structures.

Figure 9 describes the fabrication process and the suggested mechanism. Plasma activation species reinforce polymer chain scissions and introduce reactive radicals or groups. The rough surface and polar functional groups become attractive to phosphorus–fluoride emulsion molecules, resulting in improved absorption and penetration of the proposed phosphorus–fluoride component on the fabric surface [50]. More molecules tangle with the rough surface, and the carboxyl or hydroxyl groups consequently form an adhesive coating on the fiber surface of aramid. Therefore, the durable flame-resistant ultra-hydrophobic surface was obtained.

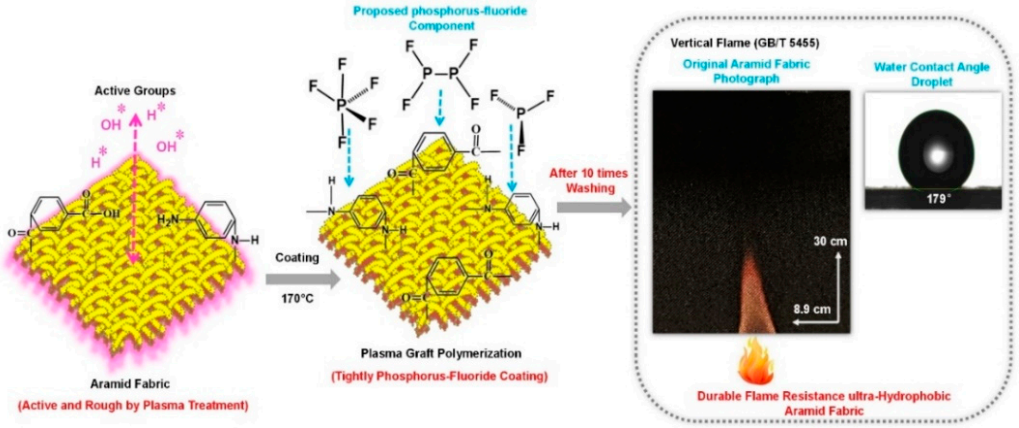

Figure 9. Suggested schematic for the mechanism of preparing a durable flame-resistant and ultra-hydrophobic aramid fabric.

4. Conclusions

We presented an efficient technique to obtain durable flame-resistant ultra-hydrophobic aramid fabric. Subsequently, after plasma treating, the coating of phosphorus–fluoride emulsion copolymer on aramid fabric by plasma graft polymerization deduces a remarkably improved flame-resistant ultra-hydrophobic on the plasma-treated coated aramid fabric. Regarding the flame test, the fabric maintained its solidity with 0.68 cm char length through no observable after-flame or after-glow times, and its water contact angle was more than 170°. After 10 repeatable washing cycles, plasma-coated fabrics still kept a static water contact angle of more than 170° and manifested a char length of 0.95 cm during 0 s after flame time and 0 s glow time. For directly coated fabric, its statistic water contact angle decreased to near the intrinsic value less than 100° and did not show any resistance to fire; the flame damage length was 10.6 cm with an observable after-flame time 2.5 s and after-glow of 2.1 s. EDS and XPS spectra displayed that the relative atom ratios P and F increased after plasma treatment, indicating that plasma reactive polar groups interact between phosphorus and fluorine elements, which inhibits the flammability and wettability. It is believable that the plasma roughness and activation on the fiber surface were beneficial for the diffusion and adhesion of the phosphorus–fluoride coating; this also kept extra phosphorus–fluoride elements on the fabric surface after repeating washing cycles and greatly improved the washing durability. Plasma pre-treatment with Ar and O_2 provided an eco-friendly coating on fabric surfaces with excellent potential and practical applications in fabricating durable, multifunctional synthetic polymer fabric.

Author Contributions: E.A.A.S., X.Y., and J.Z. planned the research, B.Y., and T.W. Resources, E.A.A.S. Writing—Original Draft Preparation. Writing—Review and Editing, E.A.A.S., Y.X., and J.Z.; Visualization, E.A.A.S., and Y.Z.; Supervision, J.Z.; Project Administration, J.Z. Funding Acquisition, J.Z., J.S. and Y.G. All authors have read and agreed to the published version of the manuscript.

Funding: The work is supported by the Fundamental Research Funds for the Central Universities (2232019A3-12) and the National Natural Science Foundation of China NSFC (No. 12075054-11875104).

Acknowledgments: The China Scholarship Council (CSC) is gratefully acknowledged. Sudan University of Science and Technology (SUST), College of Engineering, is recognized for supporting the first author.

Conflicts of Interest: The authors declare that they have no known competing for financial interests or personal relationships that could have appeared to influence the work reported in this paper.

References

1. Moiz, A.; Padhye, R.; Wang, X. Durable superomniphobic surface on cotton fabrics via coating of silicone rubber and fluoropolymers. *Coatings* **2018**, *8*, 104. [CrossRef]
2. Widodo, M.; El-Shafei, A.; Hauser, P.J. Surface nanostructuring of kevlar fibers by atmospheric pressure plasma-induced graft polymerization for multifunctional protective clothing. *J. Polym. Sci. Part B Polym. Phys.* **2012**, *50*, 1165–1172. [CrossRef]
3. Nabipour, H.; Wang, X.; Song, L.; Hu, Y. Graphene oxide/zeolitic imidazolate frameworks-8 coating for cotton fabrics with highly flame retardant, self-cleaning and efficient oil/water separation performances. *Mater. Chem. Phys.* **2020**, *256*, 123656. [CrossRef]
4. Vasiljević, J.; Čolović, M.; Čelan Korošin, N.; Šobak, M.; Štirn, Ž.; Jerman, I. Effect of Different Flame-Retardant Bridged DOPO Derivatives on Properties of in Situ Produced Fiber-Forming Polyamide 6. *Polymers* **2020**, *12*, 657. [CrossRef] [PubMed]
5. Serbezeanu, D.; Popa, A.M.; Stelzig, T.; Sava, I.; Rossi, R.M.; Fortunato, G. Preparation and characterization of thermally stable polyimide membranes by electrospinning for protective clothing applications. *Text. Res. J.* **2015**, *85*, 1763–1775. [CrossRef]
6. Luo, L.; Wu, P.; Cheng, Z.; Hong, D.; Li, B.; Wang, X.; Liu, X. Direct fluorination of para-aramid fibers 1: Fluorination reaction process of PPTA fiber. *J. Fluor. Chem.* **2016**, *186*, 12–18. [CrossRef]
7. Chen, X.; Wang, W.; Jiao, C. A recycled environmental friendly flame retardant by modifying para-aramid fiber with phosphorus acid for thermoplastic polyurethane elastomer. *J. Hazard. Mater.* **2017**, *331*, 257–264. [CrossRef]
8. Fu, J.; Yang, F.; Chen, G.; Zhang, G.; Huang, C.; Guo, Z. A facile coating with water-repellent and flame-retardant properties on cotton fabric. *New J. Chem.* **2019**, *43*, 10183–10189. [CrossRef]
9. Ipekci, H.H.; Arkaz, H.H.; Onses, M.S.; Hancer, M. Superhydrophobic coatings with improved mechanical robustness based on polymer brushes. *Surf. Coat. Technol.* **2016**, *299*, 162–168. [CrossRef]
10. Qian, X.; Song, L.; Bihe, Y.; Yu, B.; Shi, Y.; Hu, Y.; Yuen, R.K. Organic/inorganic flame retardants containing phosphorus, nitrogen and silicon: Preparation and their performance on the flame retardancy of epoxy resins as a novel intumescent flame retardant system. *Mater. Chem. Phys.* **2014**, *143*, 1243–1252. [CrossRef]
11. Chen, T.; Hong, J.; Peng, C.; Chen, G.; Yuan, C.; Xu, Y.; Zeng, B.; Dai, L. Superhydrophobic and flame retardant cotton modified with DOPO and fluorine-silicon-containing crosslinked polymer. *Carbohydr. Polym.* **2019**, *208*, 14–21. [CrossRef] [PubMed]
12. Zhang, P.; Fan, H.; Tian, S.; Chen, Y.; Yan, J. Synergistic effect of phosphorus–nitrogen and silicon-containing chain extenders on the mechanical properties, flame retardancy and thermal degradation behavior of waterborne polyurethane. *RSC Adv.* **2016**, *6*, 72409–72422. [CrossRef]
13. Wei, D.; Dong, C.; Chen, Z.; Liu, J.; Li, Q.; Lu, Z. A novel cyclic copolymer containing Si/P/N used as flame retardant and water repellent agent on cotton fabrics. *J. Appl. Polym. Sci.* **2019**, *136*, 47280. [CrossRef]
14. Ren, Y.; Zhang, Y.; Gu, Y.; Zeng, Q. Flame retardant polyacrylonitrile fabrics prepared by organic-inorganic hybrid silica coating via sol-gel technique. *Prog. Org. Coat.* **2017**, *112*, 225–233. [CrossRef]
15. Chen, X.; Wang, W.; Li, S.; Jiao, C. Fire safety improvement of para-aramid fiber in thermoplastic polyurethane elastomer. *J. Hazard. Mater.* **2017**, *324*, 789–796. [CrossRef]
16. Zanini, S.; Freti, S.; Citterio, A.; Riccardi, C. Characterization of hydro-and oleo-repellent pure cashmere and wool/nylon textiles obtained by atmospheric pressure plasma pre-treatment and coating with a fluorocarbon resin. *Surf. Coat. Technol.* **2016**, *292*, 155–160. [CrossRef]
17. Ding, X.; Fang, F.; Du, T.; Zheng, K.; Chen, L.; Tian, X.; Zhang, X. Carbon nanotube-filled intumescent multilayer nanocoating on cotton fabric for enhancing flame retardant property. *Surf. Coat. Technol.* **2016**, *305*, 184–191. [CrossRef]

18. He, T.; Chen, X.; Wang, Y.; Cheng, Z.; Liu, Y.; Wang, X.; Luo, L.; Chen, Y.; Liu, X. Fabrication of durable superhydrophobic surfaces of polyester fabrics via fluorination-induced grafting copolymerization. *Appl. Surf. Sci.* **2020**, *515*, 146006. [CrossRef]
19. Xu, L.; Lai, Y.; Liu, L.; Yang, L.; Guo, Y.; Chang, X.; Shi, J.; Zhang, R.; Yu, J. The Effect of Plasma Electron Temperature on the Surface Properties of Super-Hydrophobic Cotton Fabrics. *Coatings* **2020**, *10*, 160. [CrossRef]
20. Ramamoorthy, A.; El-Shafei, A.; Hauser, P. Plasma induced graft polymerization of C6 fluorocarbons on cotton fabrics for sustainable finishing applications. *Plasma Process. Polym.* **2013**, *10*, 430–443. [CrossRef]
21. Shao, Z.-B.; Tang, Z.-C.; Lin, X.-Z.; Jin, J.; Li, Z.-Y.; Deng, C. Phosphorus/sulfur-containing aliphatic polyamide curing agent endowing epoxy resin with well-balanced flame safety, transparency and refractive index. *Mater. Des.* **2020**, *187*, 108417. [CrossRef]
22. Zhang, S.-H.; He, G.-Q.; Liang, G.-Z.; Cui, H.; Zhang, W.; Wang, B. Comparison of F-12 aramid fiber with domestic armid fiber III on surface feature. *Appl. Surf. Sci.* **2010**, *256*, 2104–2109. [CrossRef]
23. Xu, Y.; Zhang, Y.; He, T.; Ding, K.; Huang, X.; Li, H.; Shi, J.; Guo, Y.; Zhang, J. The Effects of Thermal and Atmospheric Pressure Radio Frequency Plasma Annealing in the Crystallization of TiO_2 Thin Films. *Coatings* **2019**, *9*, 357. [CrossRef]
24. Carosio, F.; Alongi, J.; Frache, A. Influence of surface activation by plasma and nanoparticle adsorption on the morphology, thermal stability and combustion behavior of PET fabrics. *Eur. Polym. J.* **2011**, *47*, 893–902. [CrossRef]
25. Yuan, H.; Wang, W.; Yang, D.; Zhou, X.; Zhao, Z.; Zhang, L.; Wang, S.; Feng, J. Hydrophilicity modification of aramid fiber using a linear shape plasma excited by nanosecond pulse. *Surf. Coat. Technol.* **2018**, *344*, 614–620. [CrossRef]
26. Huang, C.-Y.; Wu, J.-Y.; Tsai, C.-S.; Hsieh, K.-H.; Yeh, J.-T.; Chen, K.-N. Effects of argon plasma treatment on the adhesion property of ultra high molecular weight polyethylene (UHMWPE) textile. *Surf. Coat. Technol.* **2013**, *231*, 507–511. [CrossRef]
27. Siddig, E.A.; Yu, X.; Tao, H.; Ming, G.; Baojing, Y.; Tianshu, W.; Zhang, J. Plasma-induced graft polymerization on the surface of aramid fabrics with improved omniphobicity and washing durability. *Plasma Sci. Technol.* **2020**, *22*, 055503. [CrossRef]
28. Gasi, F.; Petraconi, G.; Bittencourt, E.; Lourenço, S.R.; Castro, A.H.R.; Miranda, F.d.S.; Essiptchouk, A.M.; Nascimento, L.; Petraconi, A.; Fraga, M.A. Plasma Treatment of Polyamide Fabric Surface by Hybrid Corona-Dielectric Barrier Discharge: Material Characterization and Dyeing/Washing Processes. *Mater. Res.* **2020**, *23*. [CrossRef]
29. Amel, E.E.; Ying, G.; Jianjun, S.; Ke, D.; Jing, Z. Synergistic Effect of Atmospheric Pressure Plasma Pre-Treatment on Alkaline Etching of Polyethylene Terephthalate Fabrics and Films. *Plasma Sci. Technol.* **2016**, *18*, 346. [CrossRef]
30. Molina, J.; Fernández, J.; Fernandes, M.; Souto, A.P.; Esteves, M.; Bonastre, J.; Cases, F. Plasma treatment of polyester fabrics to increase the adhesion of reduced graphene oxide. *Synth. Met.* **2015**, *202*, 110–122. [CrossRef]
31. Dinçmen, M.G.; Hauser, P.J.; Gürsoy, N.Ç. Plasma induced graft polymerization of a fluorocarbon monomer on polyamide 6, 6 fabrics. *J. Text. Appar. Tekst. Konfeksiyon* **2017**, *27*, 38–45.
32. Jeong, E.; Lee, B.H.; Doh, S.J.; Park, I.J.; Lee, Y.-S. Multifunctional surface modification of an aramid fabric via direct fluorination. *J. Fluor. Chem.* **2012**, *141*, 69–75. [CrossRef]
33. Malshe, P.; Mazloumpour, M.; El-Shafei, A.; Hauser, P. Multi-functional military textile: Plasma-induced graft polymerization of a C6 fluorocarbon for repellent treatment on nylon–cotton blend fabric. *Surf. Coat. Technol.* **2013**, *217*, 112–118. [CrossRef]
34. Zhang, D.; Williams, B.L.; Shrestha, S.B.; Nasir, Z.; Becher, E.M.; Lofink, B.J.; Santos, V.H.; Patel, H.; Peng, X.; Sun, L. Flame retardant and hydrophobic coatings on cotton fabrics via sol-gel and self-assembly techniques. *J. Colloid Interface Sci.* **2017**, *505*, 892–899. [CrossRef]
35. Kamlangkla, K.; Hodak, S.K.; Levalois-Grützmacher, J. Multifunctional silk fabrics by means of the plasma induced graft polymerization (PIGP) process. *Surf. Coat. Technol.* **2011**, *205*, 3755–3762. [CrossRef]
36. Wang, S.; Liu, X.; Wang, L.; Wen, Q.; Du, N.; Huang, J. Formation mechanism and properties of fluoride–phosphate conversion coating on titanium alloy. *RSC Adv.* **2017**, *7*, 16078–16086. [CrossRef]

37. Luo, J.; Wu, Q.; Huang, H.-C.; Chen, J.-J. Studies of fluorinated methylacrylate copolymer on the surface of cotton fabrics. *Text. Res. J.* **2011**, *81*, 1702–1712.
38. Zhao, F.-G.; Zhao, G.; Liu, X.-H.; Ge, C.-W.; Wang, J.-T.; Li, B.-L.; Wang, Q.-G.; Li, W.-S.; Chen, Q.-Y. Fluorinated graphene: Facile solution preparation and tailorable properties by fluorine-content tuning. *J. Mater. Chem. A* **2014**, *2*, 8782–8789. [CrossRef]
39. Siow, K.S.; Britcher, L.; Kumar, S.; Griesser, H.J. Deposition and XPS and FTIR analysis of plasma polymer coatings containing phosphorus. *Plasma Process. Polym.* **2014**, *11*, 133–141. [CrossRef]
40. Peng, B.; Xu, Y.; Liu, K.; Wang, X.; Mulder, F.M. High-Performance and Low-Cost Sodium-Ion Anode Based on a Facile Black Phosphorus−Carbon Nanocomposite. *ChemElectroChem* **2017**, *4*, 2140–2144. [CrossRef]
41. Li, J.; Tong, W.; Yi, L. Flame-retardant composite coatings for cotton fabrics fabricated by using oxygen plasma-induced polymerization of vinyl phosphonic acid/cyclotetrasiloxane. *Text. Res. J.* **2019**, *89*, 5053–5066. [CrossRef]
42. Jesuarockiam, N.; Jawaid, M.; Zainudin, E.S.; Thariq Hameed Sultan, M.; Yahaya, R. Enhanced thermal and dynamic mechanical properties of synthetic/natural hybrid composites with graphene nanoplateletes. *Polymers* **2019**, *11*, 1085. [CrossRef]
43. Villar-Rodil, S.; Martínez-Alonso, A.; Tascón, J. Studies on pyrolysis of Nomex polyaramid fibers. *J. Anal. Appl. Pyrolysis* **2001**, *58*, 105–115. [CrossRef]
44. Shen, M.-Y.; Chen, W.-J.; Kuan, C.-F.; Kuan, H.-C.; Yang, J.-M.; Chiang, C.-L. Preparation, characterization of microencapsulated ammonium polyphosphate and its flame retardancy in polyurethane composites. **2016**, *173*, 205–212. [CrossRef]
45. Edwards, B.; El-Shafei, A.; Hauser, P.; Malshe, P. Towards flame retardant cotton fabrics by atmospheric pressure plasma-induced graft polymerization: Synthesis and application of novel phosphoramidate monomers. *Surf. Coat. Technol.* **2012**, *209*, 73–79. [CrossRef]
46. Cheng, X.-W.; Guan, J.-P.; Yang, X.-H.; Tang, R.-C. Improvement of flame retardancy of silk fabric by bio-based phytic acid, nano-TiO_2, and polycarboxylic acid. *Prog. Org. Coat.* **2017**, *112*, 18–26. [CrossRef]
47. Khattab, T.A.; Mohamed, A.L.; Hassabo, A.G. Development of durable superhydrophobic cotton fabrics coated with silicone/stearic acid using different cross-linkers. *Mater. Chem. Phys.* **2020**, *249*, 122981. [CrossRef]
48. Wang, Y.; Lan, Y.; Shi, X.; Sheng, Y.; Yang, Y.; Peng, S.; Xu, J. Highly efficient fabrication of self-extinguished flame-retardant and underwater superoleophobic coatings through layer-by-layer method. *Mater. Chem. Phys.* **2020**, *256*, 123590. [CrossRef]
49. Taherkhani, A.; Hasanzadeh, M. Durable flame retardant finishing of cotton fabrics with poly (amidoamine) dendrimer using citric acid. *Mater. Chem. Phys.* **2018**, *219*, 425–432. [CrossRef]
50. Möncke, D.; Eckert, H. Review on the structural analysis of fluoride-phosphate and fluoro-phosphate glasses. *J. Non-Cryst. Solids X* **2019**, *3*, 100026. [CrossRef]